A99-33633

AIAA 99-3530

High Reynolds Number Flows: A Challenge for Experiment and Simulation

A. J. Smits
Department of Mechanical and Aerospace Engineering,
Princeton University,
Princeton, NJ 08544

and

I. Marusic
Department of Aerospace Engineering and Mechanics,
University of Minnesota,
Minneapolis, MN 55455

30th AIAA Fluid Dynamics Conference
28 June - 1 July, 1999 / Norfolk, VA

High Reynolds Number Flows: A Challenge for Experiment and Simulation

Alexander J. Smits[*]
Department of Mechanical and Aerospace Engineering
Princeton University
Princeton, New Jersey 08544-0710

and

Ivan Marusic[†]
Department of Aerospace Engineering and Mechanics
University of Minnesota
Minneapolis, MN 55455

Abstract

Most available information on the behavior of turbulent flows has been obtained using small-scale facilites and limited computer resources. Consequently, the range of Reynolds numbers over which detailed data are available is limited, and in the case of large vehicles such as aircraft and submarines, several orders of magnitude smaller than that experienced in practice. This disparity in Reynolds number places a great emphasis on scaling laws, since the variation with Reynolds number must be known very accurately before predictions of the full-scale performance can be made with confidence. In many instances, we do not know the scaling laws with sufficient precision to make acceptable predictions, and further research is required. In this paper, we discuss the uncertainties in scaling laws as we understand them at present, and suggest a number of new experiments that will shed light on this subject.

[*]Associate Fellow, AIAA
[†]Member, AIAA

1 Introduction

Research into the long standing problem of wall turbulence has in general been confined to conventional laboratory-scale facilities and restricted by limited computing capabilities. As a result, most available data are confined to low to moderately high Reynolds numbers. However, high Reynolds numbers are encountered in many practical applications and engineering calculations based on scaling laws must be applied. For example, large vehicles such as submarines and commercial transports operate at Reynolds numbers based on length of the order of 10^9, and industrial pipe flows cover a very wide range of Reynolds numbers up to 10^7. Severe economic penalties can result from the uncertainties that still exist in Reynolds number scaling. For example, for submarines and ships, the uncertain extrapolation of model results to the full-scale prototype may lead to expensive retrofits after sea trials have been completed. Similarly, the Reynolds number scaling for airframe design often leads to errors in the final design, which can incur severe financial penalties, either in reduced per-

formance or by requiring sub-optimal retro-fits such as vortex generators. In the nuclear power industry, the loss coefficient correlations for high Reynolds number pipe fittings may be subject to uncertainties as high as 50%, leading to considerable economic penalties in designing pumping systems. In addition, very important applications pertain to atmospheric and other geophysical flows where extremely high Reynolds numbers are the rule rather than the exception.

A number of recent studies have focused on establishing the correct form of the scaling laws, generating considerable debate. This is true for the mean flow (power laws versus classic logarithmic law, see [1], [2], [3]), as well as the turbulence intensities. Understanding the correct form of the scaling laws is an essential starting point for understanding the structure of the flow, for constructing turbulence models, and for predicting the performance of systems where high Reynolds numbers are encountered. Here, we present some observations regarding the Reynolds number dependence of turbulent pipe and boundary layer flows, based on recent experimental evidence obtained at Princeton and elsewhere, and we suggest new experimental approaches for future work.

2 Scaling of the Mean Flow

For wall-bounded turbulent shear flows, the shape of the mean velocity profile, or equivalently, the relative fraction of the flow occupied by the inner and outer regions, changes with Reynolds number. If the Reynolds number is large enough, it is usually assumed that the interaction between these regions vanishes because of the disparity of length scales, and consequently, independent similarity solutions may exist for each region. Therefore, most theoretical treatments start by dividing the flow into an inner and outer region. For each region, a length and velocity scale may be defined. The velocity scale in the near-wall region is typically taken to be the friction velocity. The length scale associated with the inner region is then the kinematic viscosity ν divided by the friction velocity, ν/u_τ. For the outer region, the velocity scale is also typically taken to be the friction velocity, although this has long been the source of controversy ([1], [4]), and the length scale is taken to be the radius of the pipe R or the boundary layer thickness δ.

Using dimensional analysis, the scaling for the inner region is

$$U^+ = f\left(y^+\right), \tag{1}$$

where f represents the functional dependence in the inner region [5]. Here, $U^+ = U/u_\tau$, $y^+ = yu_\tau/\nu$, y is the distance from the wall, and U is the mean velocity in the streamwise direction. Equation 1 is known as the "law-of-the-wall" and is valid only in the inner region. It can be shown from the Navier-Stokes equation that f is linear near the wall, and we may expect that equation 1 is valid further from the wall than the linear region but not into the outer region (that is, equation 1 will hold for $0 < y^+ \ll R^+$, where $R^+ = Ru_\tau/\nu$).

The dimensionless scaling law for the outer region is

$$\frac{U_{CL} - U}{u_0} = g\left(\eta\right), \tag{2}$$

where g represents the functional dependence in the outer region, and for a pipe $\eta = y/R$ and U_{CL} is the centerline velocity. The parameter u_0 is the outer velocity scale. If $u_0 = u_\tau$, then equation 2 is known as the "defect-law" [5]. Equation 2 is valid only in the outer region where viscosity is not important (that is, equation 2 will hold for $0 \ll \eta < 1$).

Equations 1 and 2 are based on the assumption that R^+ is large enough for both regions to be independent of Reynolds number. If we assume that an intermediate region exists where both scaling laws are valid, then we can define two different matching conditions.

By matching the velocity gradients given by equations 1 and 2, we find

$$y^+ f' = -\Lambda \eta g', \tag{3}$$

where the differentiation in equation 3 is with respect to the dependent variables and Λ is the ratio of the outer to inner velocity scales, u_0/u_τ. If $u_0 = u_\tau$, then equation 3 is the same relation used by [6] to derive the classical logarithmic overlap region.

Alternatively, if we simultaneously match the velocities and velocity gradients, the matching condition is

$$y^+ \frac{f'}{f} = -\frac{\eta g'}{\frac{U_{CL}}{u_0} - g}. \quad (4)$$

Equation 4 is the same relation used by George *et al.* [1] with $u_0 = U_\infty$ to support their assertion that the overlap region in a boundary layer is given by a power law.

At low Reynolds numbers that are still high enough that an overlap region exists, we expect that Λ depends on R^+. At these Reynolds numbers, equation 3 does not define an overlap region that is independent of R^+, but equation 4 does. By integrating equation 4, the velocity profile in this region can be written using inner layer variables as

$$U^+ = C_1 \left(y^+\right)^\gamma. \quad (5)$$

3 Turbulent Pipe Flow

To verify these scaling concepts, pipe flow measurements were obtained in the Princeton/DARPA-/ONR Superpipe apparatus which can achieve a range of Reynolds numbers spanning three orders-of-magnitude. The facility uses compressed air as the working fluid to achieve very high Reynolds numbers at a reasonable cost. A closed-loop system was built with the test pipe located inside high-pressure piping (see figure 1). The test pipe had a nominal diameter of $129\,mm$, with a length-to-diameter ratio of 200. Very high-pressure air (up to 200 atmospheres) is used to achieve the high Reynolds numbers. The wall is polished smooth over its full length to a roughness measure of approximately 0.15 μm rms. Further details of the facility are given in [4], [3] and [7].

The results show that the values of C_1 and γ were independent of Reynolds number and equal to 8.70 and 0.137, respectively (see figure 2a). Equation 5 with these constants was shown to be in excellent agreement with pipe flow data for $60 < y^+ < 500$ or $y^+ < 0.15R^+$, the outer limit depending on whether R^+ is greater or less than 9×10^3 [3]. With these limits, a power law can exist only if $R^+ > 400$.

At even higher Reynolds numbers, it was shown that u_0/u_τ approaches a finite limit [4]. For this case, equation 3 also gives an overlap region which is independent of Reynolds number. Equation 3 can be set equal to a constant (typically $1/\kappa$) and integrated to give the classical log law which can be written in terms of inner scaling variables as

$$U^+ = \frac{1}{\kappa} \ln y^+ + B. \quad (6)$$

The values of κ and B were found to be 0.436 and 6.15, and as shown in figure 2b this log law is in excellent agreement with experimental pipe flow data for $600 < y^+ < 0.07R^+$ [3]. With these limits, a log law can exist only if $R^+ > 9 \times 10^3$ which is a very large Reynolds number compared to most laboratory flows.

For the preceding argument to be valid, u_0 must be proportional to u_τ at high Reynolds number. The correct velocity scale for the outer region was shown to be the velocity deficit in the pipe, or $U_{CL} - \bar{U}$, where $\bar{U}$ is the average velocity, which is a true outer velocity scale, in contrast to the friction velocity which is a velocity scale associated with the inner region which is "impressed" on the outer region [4]. The comparisons with the data are shown in figure 3. As expected on the basis of the argument given here, the collapse of the data for $y/R > 0.1$ using u_0 is considerably better than that using u_τ.

4 Turbulent Boundary Layers

The preceding analysis for pipe flow may also hold for boundary layers if the centerline velocity is replaced by the freestream velocity and the radius is replaced by the boundary layer thickness [8]. Here we also assume that the streamwise dependence of the velocity profile is properly accounted for by our choice of length and velocity scales. An outer velocity scale equivalent to $U_{CL} - \bar{U}$ can be expressed using boundary layer parameters as follows.

$$\begin{aligned} u_0 &= U_\infty - \bar{U} = \frac{U_\infty}{\delta} \int_0^\infty \left(1 - \frac{U}{U_\infty}\right) dy \\ &= U_\infty \frac{\delta^*}{\delta}. \end{aligned} \quad (7)$$

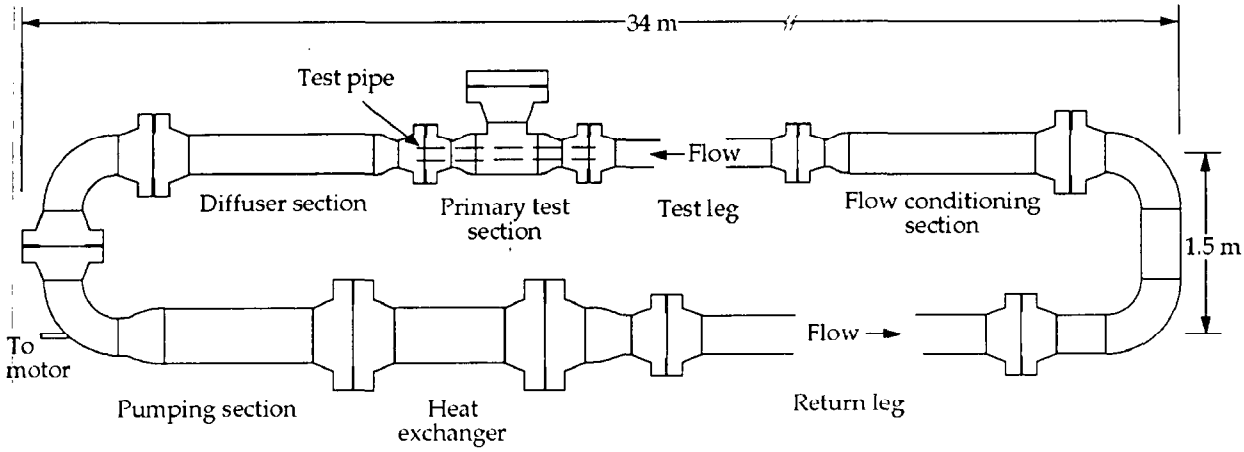

Figure 1: The layout of the SuperPipe facility. The flow direction is counter-clockwise.

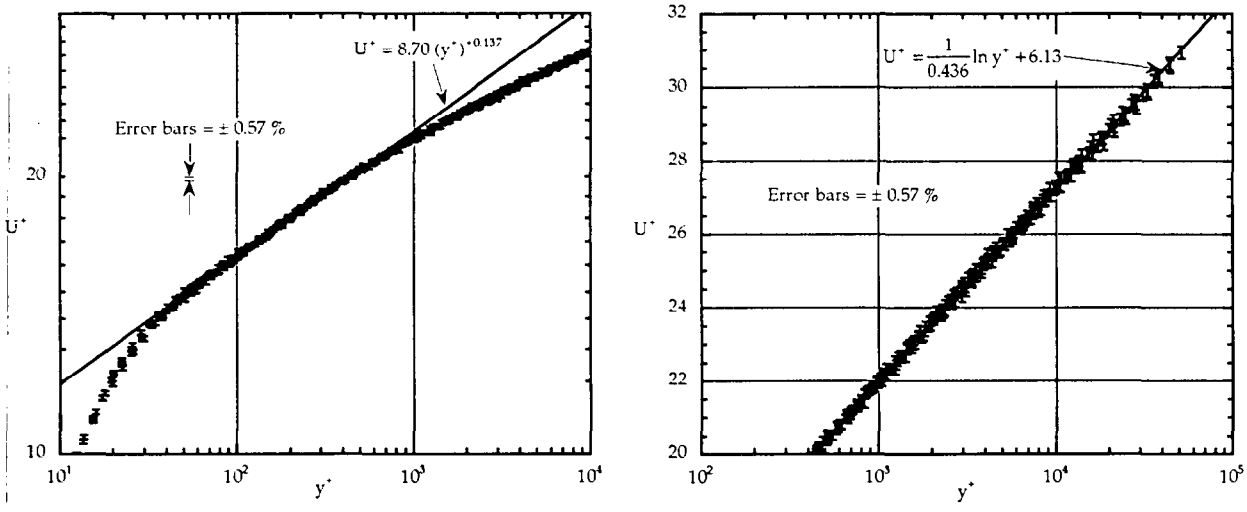

Figure 2: Pipe flow velocity profiles normalized using inner scaling variables for 26 different Reynolds numbers between 31×10^3 to 35×10^6 [4]. (a) Log-log plot; (b) Linear-log plot.

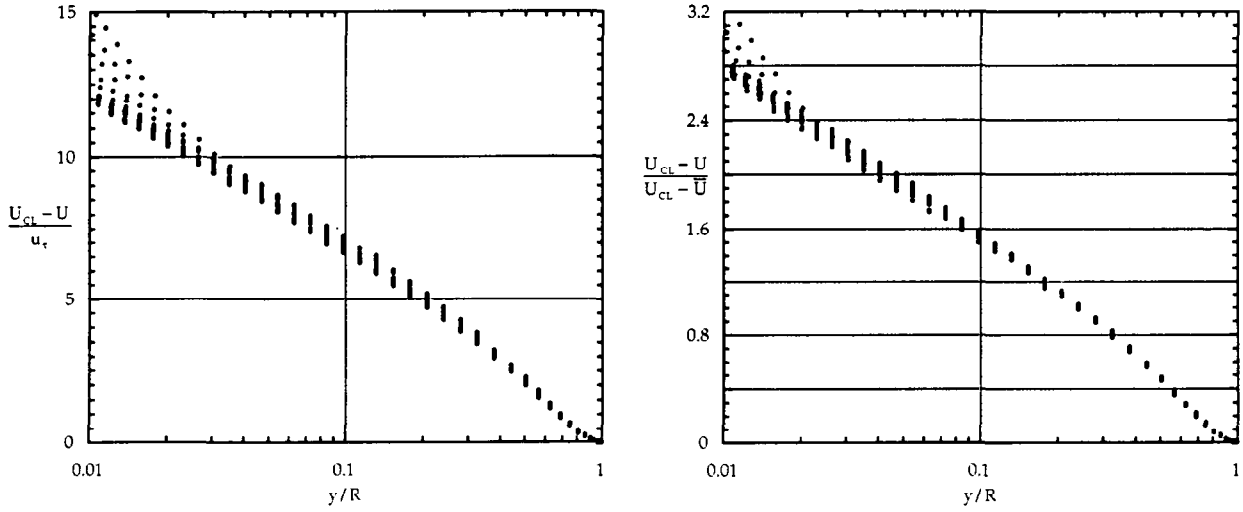

Figure 3: Pipe flow velocity profiles for Reynolds numbers between 31×10^3 to 35×10^6 [4]. (a) Normalized using the conventional outer velocity scale; (b) Normalized using the proposed new outer velocity scale.

This new outer velocity scale can be accurately determined from the velocity profiles, in contrast to the friction velocity u_τ which is not easily measured accurately in a boundary layer. The new outer velocity scale is related to the Clauser or Rotta thickness Δ which is given by

$$\Delta = \int_0^\infty \frac{U_\infty - \bar{U}}{u_\tau}\, dy = \delta^* \sqrt{\frac{2}{C_f}},$$

so that

$$u_0 = U_\infty \frac{\delta^*}{\delta} = u_\tau \sqrt{\frac{2}{C_f}} \frac{\delta^*}{\delta} = u_\tau \frac{\Delta}{\delta}. \qquad (8)$$

At high Reynolds numbers, we can expect that $u_0 \propto u_\tau$, or equivalently $\delta^*/\delta \propto \sqrt{C_f}$, (or $\Delta \propto \delta$) for a logarithmic overlap region to exist (the skin friction coefficient $C_f = 2(u_\tau/U_\infty)^2$).

An approximate basis for comparison between pipe and boundary layer flows is to estimate the equivalent momentum thickness of a fully-developed pipe flow at about 1/10th the radius, so that the equivalent value of $Re_\theta \approx Re_D/20$. However, comparisons between boundary layers and pipe flows must be made very carefully. Even though a similar scaling may exist for boundary layers and pipe flow, we can not expect the functional form of the velocity profiles in the outer region $g(\eta)$ to be the same since the equations of motion and the boundary conditions are different. This is true even in the infinite Reynolds number limit. Furthermore, any limit that depends on Reynolds number (R^+ or δ^+) may be different due to the differences in the outer region (here $\delta^+ = \delta u_\tau/\nu$). These limits include the Reynolds number at which complete similarity exists in the outer and inner region, the outer limit of the power law or log law, and the Reynolds number at which the overlap regions appear. Conversely, the equations of motion and boundary conditions of the inner region are the same for both flows in the infinite Reynolds number limit, and we may therefore expect that the functional form of the velocity profiles in the inner region $f(y^+)$ are the same.

Data from three separate boundary layer investigations were used for the comparison presented here. The data from Purtell *et al.* [9] spanned the range $470 < Re_\theta < 5,100$ ($220 < \delta^+ < 1,700$); the data from Smith [10] spanned the range $4,600 < Re_\theta < 13,00$ ($1,500 < \delta^+ < 4,000$); and the data from Fern-

holz *et al.* [42] provided the data at $Re_\theta = 21,000$ and 58,000 ($\delta^+ = 6,900$ and 18,000).

In figure 4, the velocity profiles reported in [9], [10] and [42] are shown normalized by inner layer variables. The data at values of $\delta^+ < 500$ are not shown since it is doubtful that a universal overlap region exists at these Reynolds numbers. The power law established from pipe flow data is also shown, as are the regions marking a $\pm 3\%$ error in u_τ (representing a best estimate for the uncertainty in u_τ). For all profiles except at the highest Reynolds number, the data are nominally within $\pm 3\%$ of the power law for some range of y^+ and deviate from the curve in the inner region where viscosity dominates and in the outer region where the inner scaling no longer holds. At the highest Reynolds number, the data near the wall deviates from the other profiles by more than 3%, but this perhaps can be attributed to an error in position since the five points nearest to the wall are all within 1 mm of the wall. The log law established from pipe flow data is also shown in figure 4. According to the analysis of pipe flow data, the log law should be apparent only at the highest Reynolds number since a log law should not exist until δ^+ is of order 10^4. The uncertainty in the friction velocity prevents us from drawing any definitive conclusions here, but a power law with $C_1 = 8.70$ and $\gamma = 0.137$ seems to be in good agreement with these boundary layer data.

In figures 5 and 6, the velocity profiles are normalized by the conventional outer velocity scale, u_τ, and the proposed outer velocity scale $U_\infty \delta^*/\delta$, respectively. In each figure, error bars are shown which represent a $\pm 3\%$ uncertainty of the ordinate at $y/\delta = 0.1$. When normalizing the wall-normal position in the outer region, the length scale was taken to be the boundary layer thickness at $0.99U_\infty$, although it was found that the profiles collapsed equally well when using the displacement thickness or momentum thickness. Regardless of the length scale used, the collapse is poor in the outer region for the profiles normalized by u_τ and much improved for $y/\delta > 0.07$ and for $650 < \delta^+ < 18 \times 10^3$ when using $U_\infty \delta^*/\delta$.

5 Turbulence Scaling

Many existing turbulence modeling schemes rely on the assumption of wall functions, where the turbulence intensities follow the mean-flow behavior and scale with inner-flow variables. That is, where $U/u_\tau = g(y^+)$ is approximately valid, $\overline{u_1^2}/u_\tau^2 = f_1[y^+]$, $\overline{u_2^2}/u_\tau^2 = f_2[y^+]$, $\overline{u_3^2}/u_\tau^2 = f_3[y^+]$, and so forth. Here U is the mean streamwise velocity, u_1, u_2 and u_3 are the streamwise (x), wall-normal (y) and spanwise (z) components of the fluctuating velocity respectively and overbars denote temporal averages.

A large number of studies have now emerged which strongly contest such thinking. In line with this, Marusic *et al.* [12] proposed a similarity law for the streamwise turbulence intensity which predicts that the level of $\overline{u_1^2}/u_\tau^2$ should increase monotonically with increasing Reynolds number, in the turbulent wall region, e.g. for say, $y^+ \geq 100$; $y/\delta < 0.15$.

Existing experimental data show support for this formulation which is consistent with Townsend's attached eddy hypothesis. However, these studies have all been at conventional laboratory scales and it is unclear whether or not this formulation is valid at very high Reynolds numbers and to what limit this idea can be extended. For the other components of Reynolds stress ($\overline{u_2^2}$, $\overline{u_3^2}$, $-\overline{u_1 u_2}$) the Reynolds number scaling issue remains even more unclear.

To address these issues, and the structure of high Reynolds number wall turbulence in general, the need clearly exists for high quality turbulence measurements in high Reynolds number boundary layers. By "high" we mean $\delta^+ = O(10^5)$, where $\delta^+ = \delta u_\tau/\nu$.

There is an urgent need for research to quantify, in precise terms, the Reynolds number scaling laws for the Reynolds stress tensor $\overline{u_i u_j}$ in canonical turbulent boundary layers. To achieve this, three unique and complementary high Reynolds number facilities are now available, which together can provide a complete picture of the wall turbulence across the entire layer. The first is in the atmospheric boundary layer on the salt-flats of Utah at the SLTEST facility. The SLTEST (Surface Layer Turbulence and Environmental Science Test) facility provides an environment suitable for mimicking wind tunnel-like conditions. This facility can provide high accuracy measurements

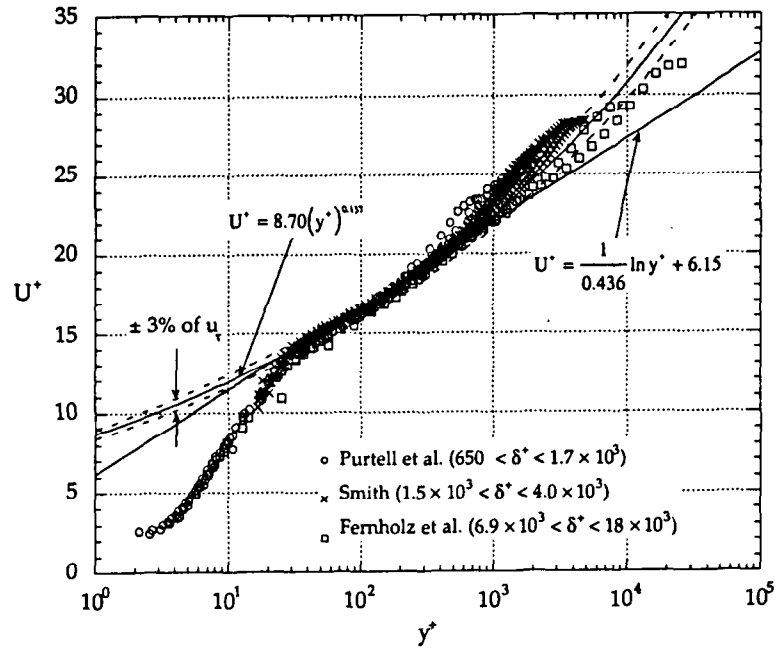

Figure 4: Boundary layer velocity profiles normalized using inner scaling variables.

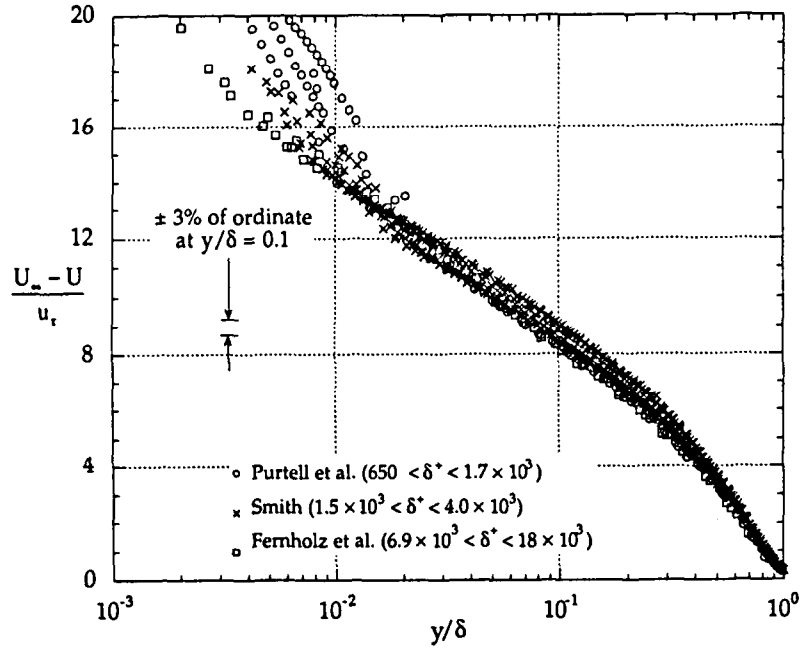

Figure 5: Boundary layer velocity profiles normalized using traditional outer scaling variables.

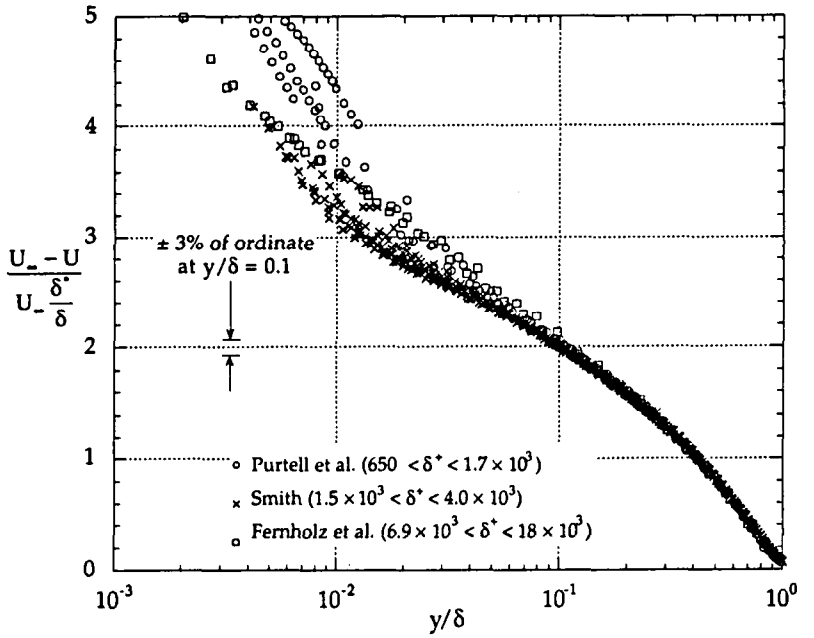

Figure 6: Boundary layer velocity profiles normalized using proposed outer scaling variables.

in the region near the wall, $2 \leq y^+ \leq O(5,000)$, where $\delta^+ = O(5 \times 10^5)$.

The second high Reynolds number test facility is is the Princeton Superpipe. The Princeton Superpipe generates Reynolds numbers of the same order as the atmospheric boundary layer flow. Measurements in the overlapping range of y^+ in the wall region, between the two flows, will allow a definitive test of the notion of "wall universality." Also, results from our preliminary studies show that the turbulence intensities can be compared between boundary layers and pipe and channel flows, even in the outer region of the flow. This is based on a formulation using Townsend's Reynolds number similarity hypothesis.

The third is the High Reynolds Number Testing Facility (HRTF) at Princeton, which also uses compressed air as the working fluid. The facility, shown in figure 7, is funded by ONR, and it is designed to study lift and drag, wake formation and decay, unsteady flows typical of maneuvering vehicles, turbulence in boundary layers and wakes, at Reynolds numbers typical of full-scale ships, submarines, torpedos and airplanes (up to length Reynolds number of 176×10^6). There are two working sections, each is 8 ft long with an internal diameter of 18 in. This facility is expected to provide vital new data on the performance of submarines and torpedoes, as well as providing a new capability for minimizing risks in the development of new and innovative vehicles. It can also be used for fundamental studies of turbulent flows at high Reynolds numbers, specifically turbulent boundary layers up to $Re_\theta = 250,000$. The HRTF may be used to verify the mean flow scaling proposed by Zagarola & Smits [8], and the outer-layer turbulence scaling proposed by Marusic *et al.* [12], as well as verify the concept of wall universality.

In what follows, we discuss the present state of knowledge of scaling laws for wall turbulence highlighting existing anomalies. We then propose specific research studies, together with a discussion on relevant measurement accuracy issues and how they can be addressed.

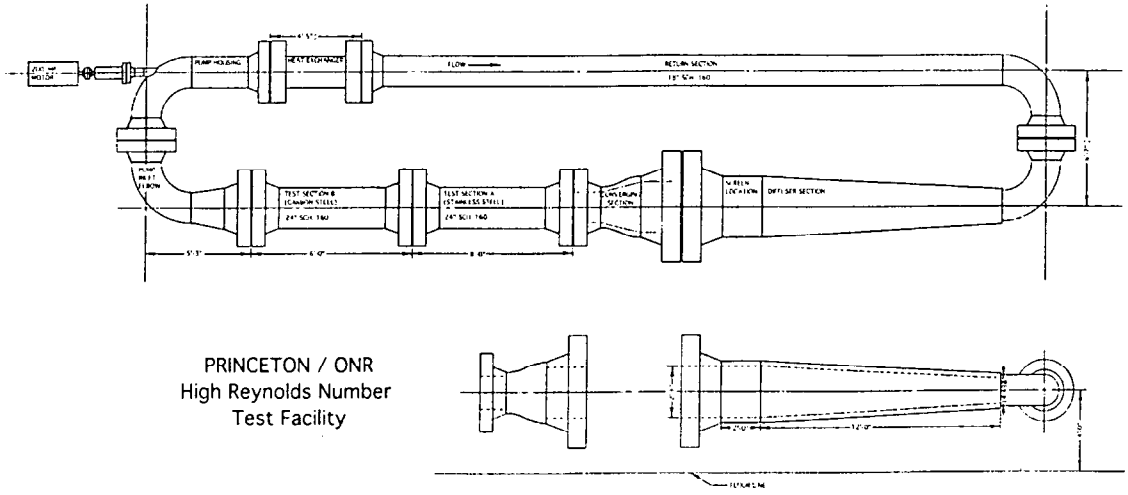

Figure 7: The High Reynolds Number Testing Facility at Princeton University.

6 Scaling Laws for Wall Turbulence

In recent reviews of experimental data, there has been considerable discussion on the applicability of scaling laws to the streamwise turbulence intensity ($\overline{u_1^2}$). (Limited discussion of other turbulence quantities is probably due to the shortage of reliable measurements). Gad el Hak & Bandyopadhyay[13] and Fernholz & Finley [14] reviewed zero-pressure-gradient turbulent boundary layers and noted evidence of strong Reynolds number effects on $\overline{u_1^2}$ when normalized using inner-wall variables. By inner scaling we mean $\overline{u_1^2}/u_\tau^2 = f[y^+]$ while outer scaling involves normalization with the length scale δ. Mochizuki & Nieuwstadt [15] surveyed a large collection of experimental data in both conventional flat plate boundary layers and in pipes and ducts and specific attention was given to whether the peak in $\overline{u_1^2}$, which occurs at $y^+ \approx 15$, is Reynolds number independent. Variations between different experiments of this value for $\overline{u_1^2}/u_\tau^2$ were $\pm 10\%$ but the variation was concluded not to be statistically significant. Coles [16] also surveyed a large numbers of wall-bounded flow experiments and arrived tentatively at the same conclusion. Fernholz & Finley [14] suggest that a weak Reynolds number effect may be present but like Coles, draw attention to the difficulty of reaching firm conclusions in the presence of the significant scatter in the data. Mochizuki & Nieuwstadt further concluded that $\overline{u_1^2}$ does scale with inner-flow variables in the entire wall region (we understand this to be from $y^+ = 0$ to $y/\delta \leq 0.15$, say) which agrees with the approach taken by many conventional computational turbulence models where the existence of inner-layer scaling is assumed for all components of the Reynolds stress tensor and mean-flow velocity. Smits & Dussauge [17] and Dussauge *et al.* [18] also reviewed the data presented in [14] and arrived at the conclusion that for a high enough Reynolds number the $\overline{u_1^2}$ profiles display similarity in the viscous sublayer and buffer layer in inner scaling, while similarity in outer scaling is observed in the mean-flow logarithmic layer and the remainder of the outer region.

Doubts as to the validity of inner-flow scaling in the near-wall region have recently been raised in [19] and [20] from studies of computational DNS results. Durst *et al.* [21] made LDA measurements in a low-Reynolds-number pipe flow and also concluded that turbulence intensities in the wall region do not scale with inner variables. However, they note that very

close to the wall only a weak Reynolds number dependence exists. For $y^+ \leq 15$ they believe their data, within experimental uncertainty, scales with inner variables.

Marusic *et al.* [12] proposed a similarity law for $\overline{u_1^2}$ for zero-pressure-gradient wall turbulence, formulated for the region of the flow above the viscous buffer zone, that is, $y^+ \geq 100$ and $y/\delta \leq 1$. The formulation is based on the attached eddy hypothesis, as extended by Perry & Marusic [22] and Marusic & Perry [23] and the Reynolds-number-similarity hypothesis [24]. A further assumption is made of the existence of Kolmogorov eddies with a universal inertial subrange. The form of the expression is

$$\frac{\overline{u_1^2}}{u_\tau^2} = B_1 - A_1 \ln[\frac{y}{\delta}] - V_g[y^+] - W_g[\frac{y}{\delta}], \quad (9)$$

where A_1 and B_1 are universal constants (for fully developed zero pressure gradient layers), V_g is a correction term for the Kolmogorov and attached eddy cut-off where $V_g \rightarrow 0$ for y^+ sufficiently large and W_g is a term analogous to the mean flow Coles wake function where $W_g \rightarrow 0$ for y/δ sufficiently small. This is shown schematically in figure 8. In figure 9, a comparison between existing experimental data and the formulation is shown and good agreement is observed. Also shown on this figure is the predicted profile for $\delta^+ = \delta u_\tau/\nu = 5 \times 10^5$. This is the range of Reynolds number that will be considered in the proposed research. Going to such a high Reynolds number should provide a definitive test for equation 9.

The most significant implication of equation 9 is that the level of $\overline{u_1^2}/u_\tau^2$ at $y^+ = O(200)$, say, continues to rise with Reynolds number without limit. This trend implies that with increasing δ^+ then $(\overline{u_1^2}/U^2)_{y^+=200}$ (where U is the local mean velocity) will increase without limit. This ultimately must lead to momentary flow reversals occurring. At first glance, it would appear that the formulation might "self destruct" at sufficiently high Reynolds numbers because of this. Nevertheless, from work by Perry & Chong [25] which considers the flow topology of turbulent boundary layers near the wall, momentary flow reversals were shown to occur even in the zero-pressure-gradient flow case [26], at least at $y^+ \rightarrow 0$. These observations come from studying streamline and vortex line patterns. The same work also shows that in adverse-pressure-gradient layers, such momentary flow reversals in localized regions are very common, as seen in the data of [27], at least at $y^+ \rightarrow 0$, even though the flow in the mean is attached. It could well be that the similarity law is still valid even with such flow reversals. In the absence of high Reynolds number measurements, how far this formulation can be extended is not known.

6.1 Implications for near-wall region

The other striking feature of the $\delta^+ = 5 \times 10^5$ prediction is that the level of $\overline{u_1^2}/u_\tau^2$ exceeds the peak turbulence intensity at $y^+ \approx 15$. In such an event, it is difficult to see how inner-flow scaling could be valid for $\overline{u_1^2}$. The implications of scaling trends for the other components of turbulence intensity can also be considered using the attached eddy hypothesis, which is main theory behind equation 9. For example, in the case of the wall-normal componet ($\overline{u_2^2}$), the attached eddy hypothesis would imply that $\overline{u_3^2}/u_\tau^2$ remains invariant with Reynolds number in the wall-region. The explanation behind this is also related to the notion of "inactive motions" as discussed in [28] and [29]. These are large-scale motions which contribute to the streamwise and spanwise broadband-turbulence intensities near the wall but not the wall-normal turbulence intensity and Reynolds shear stress. Townsend [29] points out that these "motions" can be fully described by the presence of attached eddies and this is incorporated in the attached eddy model of [22]. Here the main energy-containing motions of the boundary layer are described by superimposing the contributions from a range of scales of geometrically similar representative eddies, and the contribution of one scale of eddies of length scale δ_e to $\overline{u_1^2}/u_\tau^2$ is proportional to $I_{11}[y/\delta_e]$, the streamwise Townsend eddy intensity function. By Taylor series expanding the velocity field for inviscid boundary conditions, Townsend [30] deduced that I_{11} must approach a constant as $y/\delta_e \rightarrow 0$, whereas it rapidly decays to zero for increasing y/δ_e for $y/\delta_e > 1$. This directly implies that all eddies with length scale $\delta_e > O(y)$ will have con-

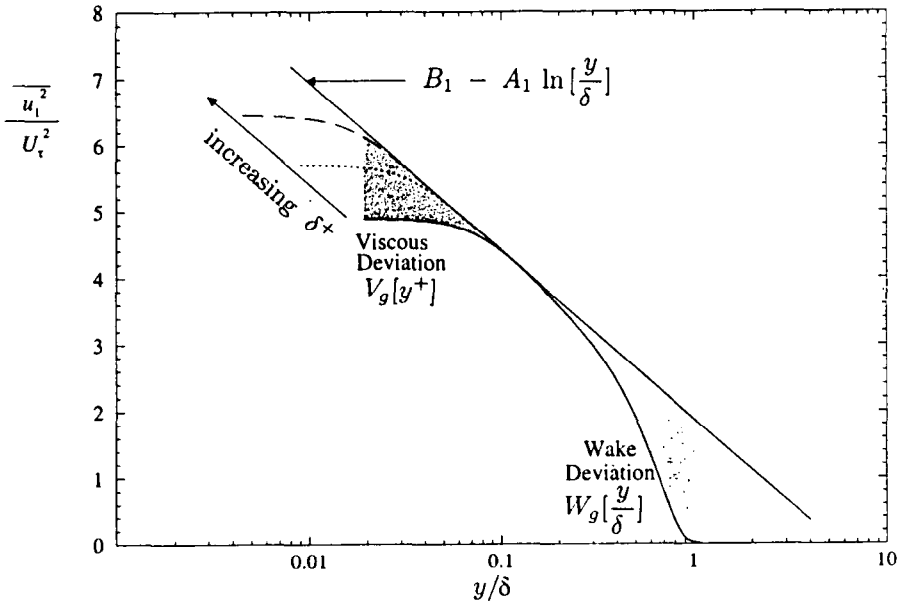

Figure 8: A mean-flow velocity-defect analogous picture for the streamwise broadband-turbulence intensity for flow above the viscous buffer zone ($y^+ \geq 100$).

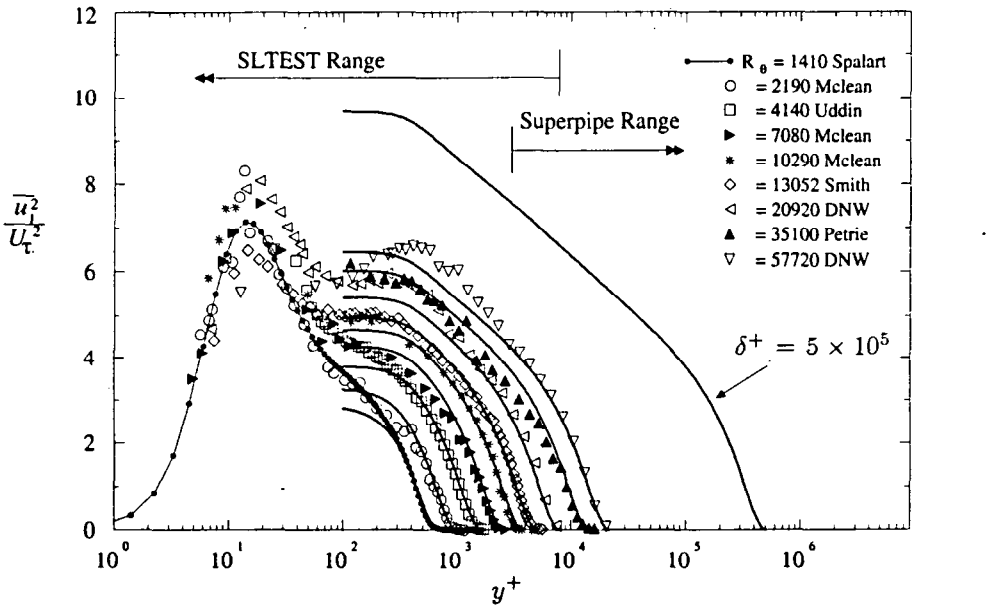

Figure 9: Similarity equation 9 (solid lines) compared to zero pressure gradient boundary layer data (taken from Marusic *et al.* 1997), and prediction for $\delta^+ = \delta\ u_\tau/\nu = 5 \times 10^5$ as expected for SLTEST and Superpipe flows.

tributions to $\overline{u_1^2}/u_\tau^2$ at this y-position and this results in the "inactive motions." This also applies to the intensity function $I_{33}[y/\delta_e]$, and hence $\overline{u_3^2}/u_\tau^2$, the spanwise intensity. This is not true for I_{22} and I_{12} which fall to zero as $y/\delta_e \to 0$. As the Reynolds number increases, the range of eddy length scales δ_e increases and so $\overline{u_1^2}/u_\tau^2$ and $\overline{u_3^2}/u_\tau^2$ keep increasing but $\overline{u_2^2}/u_\tau^2$ and $-\overline{u_1 u_2}/u_\tau^2$ asymptote to a finite universal limit above the buffer zone. (It is important to restate that this only applies for the region above the viscous buffer zone where inviscid boundary conditions apply and the motions can be thought of as a "meandering and swirling" of the fluid in the streamwise-spanwise plane).

Considering these trends, it would seem reasonable to speculate that the influence of these "inactive motions" is the following. Since the intensities $\overline{u_1^2}/u_\tau^2$ and $\overline{u_3^2}/u_\tau^2$ increase with increasing Reynolds number, above the buffer zone, it is likely that these components *will not show inner scaling* in the viscous sublayer and buffer zone. Conversely, since $\overline{u_2^2}/u_\tau^2$ and $-\overline{u_1 u_2}/u_\tau^2$ retain universal values invariant with y^+ for $y/\delta \to 0$ above the buffer zone for increasing Reynolds numbers, it is likely that these quantities *will show inner scaling* in the viscous sublayer and buffer zone.

The above predictions are not likely to be valid if the Reynolds number is not sufficiently large, since the ratio of the largest to smallest attached eddies is proportional to $\delta^+ = \delta u_\tau/\nu$. Restricting measurements to low-Reynolds-number flows may mean that an inadequate range of scales of attached eddies exists. This is probably the case for the low-Reynolds-number data reviewed by Bradshaw & Huang [19] where they concluded that none of the Reynolds stresses show inner-scaling. Experiments at very high Reynolds numbers are needed to resolve the issue.

6.2 Anomalies in existing data

The debate over the correct Reynolds number scaling for the turbulence intensities, is further exacerbated by preliminary measurements of streamwise turbulence intensity which have been carried out in the Princeton Superpipe [31], [32]. The data appear to show an anomalous behavior, where at Reynolds numbers greater than 500,000, the turbulence intensity (scaled according to conventional wisdom) at a given distance from the wall decreases with Reynolds number. If this behavior is indeed correct, it indicates a completely new scaling, contrary to conventional wisdom and the scaling predicted by the attached eddy hypothesis. Since there are no other pipe flow data (nor boundary layer data) at higher Reynolds numbers to verify this result, it stands or falls on the accuracy of the measurements. Two sources of possible error exist: the spatial resolution of the probes (which would tend to reduce the measured turbulence intensity) and the fact that the flow may not be fully-developed (even with $L/D = 150$) at the highest Reynolds numbers. Clearly, further experiments are needed and the complementary measurements in the SLTEST and HRTF facilities could provide the necessary comparison to the Superpipe data.

Preliminary measurements have also been carried on the Utah salt flats prior to the development of the SLTEST facility ([33], [?]) and these results indicate that $\overline{u_1^2}/u_\tau^2$ increases with Reynolds number in the turbulent wall region. However, significant scatter is observed in these early field tests, probably due to an insufficient number of realizations being obtained under difficult field conditions. recent improvements to the SLTEST facility, which was developed under an NSF Infrastructure Grant, allow more suitable conditions for accurate measurements with greatly improved on-site calibration facilities.

6.3 Outer-scaling in internal flows

In figure 9 an indication was given of the experimental range that each the SLTEST and Superpipe can cover. (These ranges have been estimated in order to obtain accurate hot-wire measurements. A measuring range of approximately 1 mm $\leq y \leq$ 1.5 m is assumed for the SLTEST flow and approximately 0.5 mm $\leq y \leq$ (63.5 mm $= \delta$) for the Superpipe). In this way, it is seen that experiments in both facilities are required in order to give a complete picture of the wall turbulence. Clearly, it will be possible to evaluate the scaling law trends with these proposed experiments. However, for a quantitative comparison to be made between the turbulence intensities

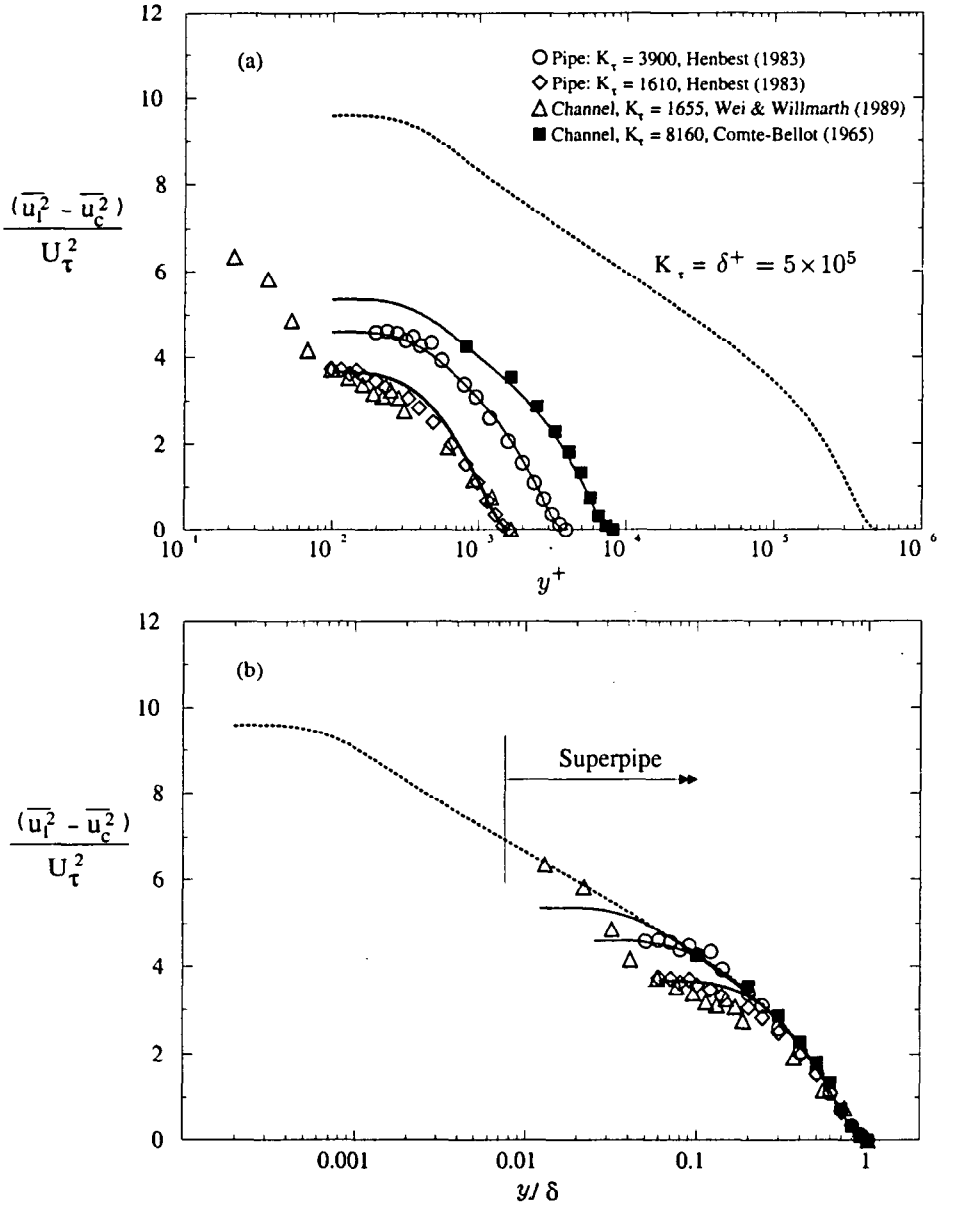

Figure 10: Experimental data in turbulent pipe and channel flow where centerline turbulence intensity ($\overline{u_c^2}/u_\tau^2$ at $y = \delta$) has been subtracted. (a) Inner-flow scaling. (b) Outer-flow scaling. Solid lines are using equation 9 where only the characteristic constant B_1 has been altered. Here $B_1 = 2.0$ ($B_1 = 2.39$ for boundary layer data in figure 9).

of the two flows in the outer part of the flow, some further rationale is required. Some preliminary work on this issue suggests that should be possible. The obvious difference between an unrestricted boundary layer flow, such as in the SLTEST facility, and a fully-developed flow, as found in pipes and channels, is that at the edge of the layer $y = \delta$, $\overline{u_1^2} = 0$ in the boundary layer while $\overline{u_1^2}$ is finite (equal to $\overline{u_c^2}$ say) for the pipe or channel (here δ is the pipe radius or channel half-width). Our preliminary results show that subtracting off the centerline turbulence intensity gives a favorable agreement with the original similarity equation 9, as shown in figure 10. As indicated, these results are of a preliminary nature, although they seem encouraging.

7 Measurement Accuracy Issues

In previous reviews [14], [35], [15], existing experimental data for $\overline{u_1^2}$, and where available $\overline{u_2^2}$, $\overline{u_3^2}$ and $-\overline{u_1 u_2}$ show a large degree of scatter, reflecting the problems of measurement accuracy in these flows. This makes it almost impossible to draw firm conclusions about Reynolds number scaling, especially given the restricted range of Reynolds numbers considered. Going to very high Reynolds numbers will certainly resolve the qualitative trends, provided the measurement errors are not excessive. However, in order to quantify this Reynolds number dependence it is essential to address two major measurement accuracy issues. The first relates to spatial and temporal resolution issues and the second to calibration procedures.

7.1 Spatial and temporal resolution

Inaccurate measurement of turbulence intensities will result when the length of the sensing element of the hot-wire is larger than the length scales of motion which contribute to the turbulence intensity. Similarly, if the sampling rate is not sufficiently fast, energy contributions will be missed from turbulence scales associated with frequencies larger then half the maximum sampling rate (based on Nyquist's sampling criterion).

One of the main advantages of the SLTEST boundary layer is the extraordinary large scales which will be encountered. The Kolmogorov length scale, η is estimated[1] to be O(1 mm) near the wall which is of the same scale of conventional hot-wire filaments. In addition, the frequencies that need to be resolved at non-dimensional wavenumber, $k_1\eta = 1$, correspond to O(1000 Hz)[2]. Therefore there will be no difficulty in resolving the turbulence fully with conventional techniques and no need to make any *a priori* assumptions such as isotropy of the high wavenumber motions. Correction schemes, such as that of Wyngaard [36] have been used extensively but up to now there has been no way to test the assumptions rigorously. These correction schemes may be tested in the SLTEST flow, and a new experimentally-based high-wavenumber correction scheme can be developed. The additional advantage of this correction scheme is that it will be obtained in a flow where there is no "f^2 noise" as discussed in [37]. This noise problem relates to conventional hot-wire anemometers and appears to be prevalent at high frequencies where low signal-to-noise ratios are present.

In the Superpipe and HRTF measurements, spatial and temporal resolution limitations will be a major issue. Here, the Kolmogorov length scale is estimated to be $O(2\mu$m) at $y = 1$ mm while at $k_1\eta = 1$, frequencies are estimated to be O(2 MHz). Using ultra-fast data acquisition hardware (sampling rate > 2 MHz) and sub-miniature probes $l = O(0.1$ mm) will help reduce the extent of the problem, but at some point high wavenumber corrections will need to be implemented. This is where the correction scheme obtained from the SLTEST results will be important.

7.2 Low-speed calibration

In the SLTEST measurements, low velocities are encountered close to the wall. At a wall-normal distance

[1]Here, $\eta^4 \approx \nu^3\kappa y/u_\tau^3$, using the assumptions that production and dissipation of turbulent kinetic energy are in balance and that $-\overline{u_1 u_2} \approx u_\tau^2$.

[2]Frequency is converted to streamwise wavenumber using Taylor's hypothesis of frozen turbulence: $k_1 = 2\pi f/U$.

of 1 mm ($y^+ \approx 4$) mean velocities of approximately 0.3 m/s can be expected. In this range, corrections are required for both the manometer and the Pitot-static tube. It is important to resolve this issue as it is in the low speed range that hot-wires are most sensitive to velocity perturbations and hence inaccurate calibrations can lead to misleading turbulence intensity measurements.

Hot-wires need to be calibrated relative to a known velocity reference. This is usually done with a Pitot-static tube and a differential pressure transducer. Unfortunately, this technique becomes difficult for velocities less than approximately 1 m/s due to the low levels of pressure difference and in general, even the highest quality pressure transducers will have some non-linear behavior at these low velocities. An additional problem also arises as the Pitot tube reading itself will require a Reynolds number correction when the Reynolds number based on the tube diameter is below approximately 100 [38].

To overcome these difficulties, the Pitot-static and the pressure transducer may be calibrated as a complete system relative to a known velocity reference. Two previously tested methods can be considered: one is based on a technique developed by Haw & Foss [39] and involves having a hot-wire attached to a pivoted arm falling under the action of gravity. The second method uses a "flying hot-wire" facility similar to the one described in [40]. It involves mounting a hot-wire to an air-bearing sled which moves back and forth in a known sinusoidal motion. In this way the speed and position of the probe are known at all times. The technique relies on the fact that the hot-wire sensitivity has a well defined peak when the velocity of the flow over the wire reaches zero. The tunnel velocity is adjusted such that on the downstream stroke, and at its mid-position when the sled is at a (negative) maximum, the hot-wire is moving at zero velocity relative to the flow. (This can be done by monitoring an oscilloscope trace or by using a digitally sampled signal). The tunnel velocity is then known to be at the same velocity as the sled. This technique was successfully implemented by Tan [41] in a study of low velocity free shear flows.

8 Summary

It has become apparent in the last few years that the widely accepted scaling arguments for turbulent wall-bounded flows need to be revised in light of new experimental results and new analysis. At the same time, new facilities have become available (for example, the Princeton Superpipe and HRTF facilities, and Utah's SLTEST facility), which offer a very large range of Reynolds numbers where new scaling concepts can be tested. Based on the current understanding of turbulent flows, we have tried to suggest experiments that make use of these new facilities to improve our understanding of the basic scaling laws of turbulent flows. This will provide more rigorous methods for extrapolating model results to the full scale prototype with greater accuracy.

Acknowledgments

The research in high Reynolds number flows is supported by ONR through grants N000014-97-1-0618, DURIP/ONR Grant N00014-98-1-0325, and N00014-99-1-0340, monitored by Drs. C. Wark and L.P. Purtell.

References

[1] George, W.K., Castillo, L., and Knecht, P. 1996. The zero pressure-gradient turbulent boundary layer. Technical Report No. TRL-153, S.U.N.Y. Buffalo.

[2] Barenblatt, G. I., Chorin, A J., Hald, O. H. and Prostokishin, V. M. 1997. Structure of the zero-pressure-gradient turbulent boundary layer. *Proc. Natl. Acad. Sci, USA*, 94:7817–7819.

[3] Zagarola, M.V. and Smits, A.J. 1998. Mean-flow scaling of turbulent pipe flow. *J. Fluid Mech.*, **373**, 33–79.

[4] Zagarola, M.V. and Smits, A.J. 1997. Scaling of the mean velocity profile for turbulent pipe flow. *Physics Review Letters*, **78** (2), 239–242.

[5] Schlichting, H. 1987. *Boundary-Layer Theory.* McGraw-Hill.

[6] Millikan, C.M. 1938. A critical discussion of turbulent flows in channels and circular tubes. *Proc. 5th Int. Congr. Appl. Mech.*, Wiley.

[7] Zagarola, M.V. 1996. *Mean flow scaling in turbulent pipe flow.* Ph.D. Thesis, Princeton University.

[8] Zagarola, M.V. and A.J. Smits, A.J. 1998a. A new mean velocity scaling for turbulent boundary layers. *ASME Paper FEDSM98-4950*, 1998.

[9] Purtell, L.P., Klebanoff, P.S. and Buckley, F.T. 1981. Turbulent boundary layers at low Reynolds number *Phys. Fluids*, **24** (5), 802–811.

[10] Smith, R.W. 1994. Effect of Reynolds number on the structure of turbulent boundary layers. Ph.D. Thesis, Princeton University, Princeton, NJ.

[11] Fernholz, H. H., Krause, E. Nockemann, M., and Schober, M. (1995. Comparative measurements in the canonical boundary layer at $Re_\theta \leq 6 \times 10^4$ on the wall of the DNW. *Phys. Fluids*, 7:1275–1281.

[12] Marusic, I., Uddin, A. K. M. and Perry, A. E. 1997. Similarity law for the streamwise turbulence intensity in zero-pressure-gradient turbulent boundary layers. *Physics of Fluids*, 9:3718–3726.

[13] Gad el Hak, M. and Bandyopadhyay, P. R. (1994. Reynolds number effects in wall-bounded turbulent flows. *Applied Mechanics Reviews*, 47(8):307–365.

[14] Fernholz, H. H. and Finley, P. J. (1996. The incompressible zero-pressure-gradient turbulent boundary layer: an assessment of the data. *Prog. Aerospace Sci.*, 32:245–311.

[15] Mochizuki, S. and Nieuwstadt, F. T. M. 1996. Reynolds-number-dependence of the maximum in the streamwise velocity fluctuations in wall turbulence. *Exp. Fluids*, 21:218–226.

[16] Coles, D. (1978. A model for flow in the viscous sublayer. In *Proc. Workshop on Coherent Structure of Turbulent Boundary Layers (Ed. Smith, C.R and Abbott, D.E.)*, Lehigh University, USA.

[17] Smits, A. J. and Dussauge, J. P. 1996. *Turbulent Shear Layers in Supersonic Flow.* AIP Press.

[18] Dussauge, J. P., Fernholz, H., Finley, P. J., Smith, R. W., Smits, A. J. and Spina, E. F. (1996. Turbulent boundary layers in subsonic and supersonic flow. AGARDograph 335.

[19] Bradshaw, P. and Huang, G. P. 1995. The law of the wall in turbulent flow. *Proc. R. Soc. Lond. A*, 451:165–188.

[20] Moser, R. D., Kim, J. and Mansour, N. N. 1999. Direct numerical simulation of turbulent channel flow up to $R_\tau = 590$. *Physics of Fluids*, 11:943–945.

[21] Durst, F., Jovanovic, J. and Sender, J. (1995. LDA measurements in the near-wall region of a turbulent pipe flow. *J. Fluid Mech.*, 295:305–335.

[22] Perry, A. E. and Marusic, I. 1995. A wall-wake model for the turbulence structure of boundary layers. Part 1. Extension of the attached eddy hypothesis. *J. Fluid Mech.*, 298:361–388, 1995.

[23] Marusic, I. and Perry, A. E. 1995. A wall-wake model for the turbulence structure of boundary layers. Part 2. Further experimental support. *J. Fluid Mech.*, 298:389–407.

[24] Townsend, A. A. 1956. *The Structure of Turbulent Shear Flow.* Cambridge University Press.

[25] Perry, A. E. and Chong, M. S. 1994. Topology of flow patterns in vortex motions and turbulence. *Applied Sci. Research*, 53:357–374.

[26] Spalart, P. R. 1988. Direct simulation of turbulent boundary layer up to $R_\theta = 1410$. *J. Fluid Mech.*, 187:61–98.

[27] Spalart, P. R. and Watmuff. J. H. 1992. Experimental and numerical study of turbulent boundary layers with pressure gradients. *J. Fluid Mech.*, 249:271–298.

[28] Bradshaw, P. 1967 The turbulence structure of equilibrium boundary layers. *J. Fluid Mech.*, 29:625–645.

[29] Townsend, A. A. 1961. Equilibrium layers and wall turbulence. *J. Fluid Mech.*, 11:97–120.

[30] Townsend, A. A. 1976. *The Structure of Turbulent Shear Flow.* Vol.2, Cambridge University Press.

[31] Schmanske, M. 1999. *Turbulence Measurements in High Reynolds Number Pipe Flow.* MSE Thesis, Princeton University.

[32] Williams, D.R. 1998. *Oganized Structures in the Outer Region of a Turbulent Pipe Flow.* MSE Thesis, Princeton University.

[33] Klewicki, J. C. and Metzger, M. M. 1996. Viscous wall region structure in high and low Reynolds number turbulent boundary layers. AIAA 96-2009.

[34] Folz, A., Ong, L. and Wallace, J. (1995. Near-wall turbulence measurements in the atmospheric surface layer. *Bull. APS*, 40:2027.

[35] Sreenivasan, K. R. 1989. The turbulent boundary layer. In *Frontiers in Experimantal Fluid Mechanics*, (ed. Gad-el-Hak) 37–61, Springer-Verlag.

[36] Wyngaard, J. C. 1968. Measurements of small scale turbulence structure with hot-wires. *J. Sci. Instrum.*, Series 2, 1:1105-1108.

[37] Saddoughi, S. and Veeravalli, S.V. 1996. Hot-wire anemometry behaviour at very high frequencies. Meas. Sci. Technol., **7**, 1297–1300.

[38] Chue, S. H. (1975. Pressure probes for fluid measurements. *Prog. Aerospace Sci.* 16:147–223.

[39] Haw, R. C. and Foss, J. F. 1990. Facility for low speed calibrations. *ASME, Proc. Symp. Heuristics of Therm. Anem., FED* vol. 97, University of Toronto, 29-33.

[40] Perry, A. E. 1982. *Hot-wire Anemometry.* Clarendon Press, Oxford.

[41] Tan, D. K. M. 1982. PhD thesis, University of Melbourne, Australia.

[42] Fernholz, H.H., Krause, E., Nockemann, M., and Schober, M. 1995. Comparative Measurements in the canonical boundary layer at $Re_{\delta 2} \leq 6 \times 10^4$ on the wall of the German-Dutch Windtunnel. *Phys. Fluids*, **7** (6), pp. 1275–1281.

[43] George, W. K. and Castillo, L. (1997. Zero-pressure-gradient turbulent boundary layer. *Applied Mech. Reviews*, 50:689–729.

[44] McLean, I. R. 1990. *The near wall eddy structure in an equilibrium turbulent boundary layer.* Ph.D. thesis, University of Southern California, USA.

[45] Panofsky, H. and Dutton, J. 1984. *Atmospheric Turbulence - Models and Methods for Engineering Applications.* Wiley.

[46] Petrie, H. L., Fontaine, A. A., Sommer, S. T. and Brungart,T. A. 1990. Large flat plate turbulent boundary layer evaluation. *Tech. Report* TM89-207, App. Res. Lab. Penn. State Univ.

[47] Uddin, A. K. M. 1994. *The structure of a turbulent boundary layer.* Ph.D. thesis, University of Melbourne, Australia.